Axial stretch-dependent cation entry in dystrophic cardiomyopathy: Involvement of several TRPs channels

Elizabeth Aguettaz, Juan José Lopez Barba, Amandine Krzesiak, Bruno Constantin, Christian Cognard, Stéphane Sebille

Axial stretch-dependent calcium increases in dystrophic cardiomyopathy: involvement of several TRPs channels

E. Aguettaz[1], J.J. Lopez Barba[2], A. Krzesiak[1], B. Constantin[2], C. Cognard[1], S. Sebille[1]

[1] Laboratoire de Signalisation et Transports Ioniques Membranaires (STIM), Equipe Transferts Ioniques et Rythmicité Cardiaque (TIRC), Université de Poitiers, 86073 POITIERS CEDEX 9, France
[2] Laboratoire de Signalisation et Transports Ioniques Membranaires (STIM), Equipe Calcium et Microenvironnement des Cellules Souches (CMCS), Université de Poitiers, 86073 POITIERS CEDEX 9, France

Corresponding author : Stéphane Sebille, ERL CNRS/Université de Poitiers n°7368, Pôle Biologie Santé Bât B36, 1 rue Georges Bonnet TSA 51106, 86073 POITIERS CEDEX 9, France
Phone : 33 549 453 767, Fax : 33 549 454 014, E-mail : stephane.sebille@univ-poitiers.fr

Abstract

In Duchenne muscular dystrophy (DMD), deficiency of the cytoskeletal protein dystrophin leads to well-described defects in skeletal muscle but also to dilated cardiomyopathy (DCM). In cardiac cells, the subsarcolemmal localization of dystrophin is thought to protect the membrane from mechanical stress. The dystrophin deficiency leads to membrane instability and a high stress-induced Ca^{2+} influx due to dysregulation of sarcolemmal channels such as stretch-activated channels (SACs). Effects of a mechanical stress on Ca^{2+} homeostasis dysregulation and the involvement of TRPs channels in the stretch responses were investigated in cardiomyocytes isolated from dystrophic *mdx* mice. Using microcarbon fibres technique, an axial stretch was applied to mimic effects of physiological conditions of ventricular filling. Study on cation influxes by the Mn^{2+}-quenching technique demonstrated a high stretch-dependent cationic influx in dystrophic cells, partially due to SACs. Moreover, the variation of intracellular calcium concentration ($[Ca^{2+}]_i$) measured by confocal imaging showed also a higher increase in *mdx* cardiomyocytes which depends on Ca^{2+} influx through SACs, enhanced by a Ca^{2+} induced Ca^{2+} release (CICR) mechanism. Involvement of TRPs channels in this excessive Ca^{2+} influx has been investigated using specific modulators and demonstrated both sarcolemma localization and an abnormal activity of TRPV2 channels.

In conclusion, TRPV2 channels are demonstrated here to play a key role in Ca^{2+} influxes and dysregulation in stretched dystrophin deficient cardiomyocytes.

Keywords: Duchenne Muscular Dystrophy, Dilated CardioMyopathy, *mdx*, mechanosensitivity, calcium, Stretch-Activated Channels, membrane stretch, TRPV2, TRPCs.

Graphical Abstract

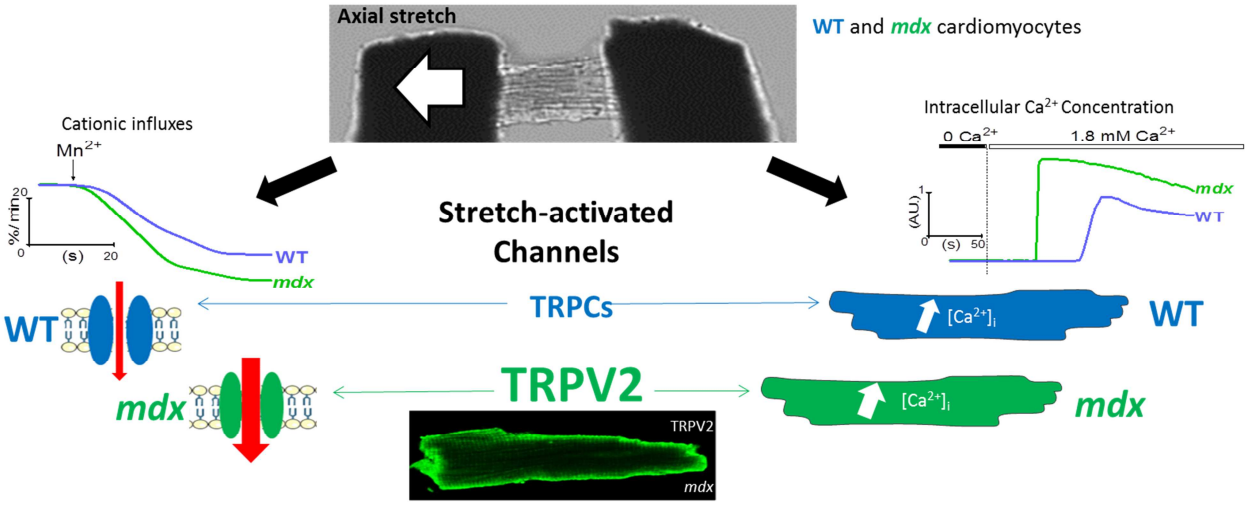

Highligths:

- Stretch-dependent cationic entries and $[Ca^{2+}]_i$ increases in cardiomyocytes
- Involvement of TRPs channels in stretch-dependent calcium responses
- TRPV2 channels play a key role in stretch-dependent calcium responses in *mdx* cells

1. Introduction

The Duchenne muscular dystrophy (DMD) is a severe X-linked disease affecting 1 in 3500 male births. Initially, DMD patients develop progressive weakness and loss the ability to walk around age 10 years. DMD is also associated by 20 years of age with cardiac complications including dilated cardiomyopathy (DCM) and arrhythmias, causing the death of about 20 % of patients [1, 2]. Mutations in the dystrophin gene on chromosome Xp21 result in the absence of the 427 kDa cytoskeletal protein dystrophin [3]. In cardiomyocytes, its subsarcolemmal and sarcomeric localization along the T-tubule network may be essential to maintain the membrane integrity [4]. This protein is also a key component of the transmembrane dystrophin-associated glycoproteins (DAG) that connects the cytoskeleton to the extracellular matrix [5]. It is thought that the lack of dystrophin leads to mechanical instability of cell membrane [6] and renders it more susceptible to rupture [7], causing elevated Ca^{2+} influx and increased susceptibility to oxidative stress [8], which activate each other in a vicious cycle that contributes to DMD pathogenesis. Several studies have suggested that the rise in intracellular Ca^{2+} is an important initiating event in the pathogenesis of dystrophic muscle [9, 10, 11]. The increased Ca^{2+} entry occurring during activity, particularly during eccentric exercise, may lead to local proteolytic activation of cationic channels and results in a further increase of Ca^{2+} entry [12].

Stretch-activated channels (SACs) are regarded as candidates for excessive Ca^{2+} influx observed in dystrophic muscles [13]. The SACs are a subcategory of mechanosensitive channels which can switch from “closed” to “open” state by stretch alone like through a direct mechanical membrane deformation (see for review: [14]). They are permeable to Na^{+}, Ca^{2+} and K^{+}, and have been suggested to be primarily involved in the pathogenesis of DMD [15; 16, 17]. Cardiac SACs can be either cation non-selective (SAC_{ns}) or potassium-selective (SAC_{k}). SAC_{ns} are thought to be localized in membrane regions that are difficult to access for patch-clamp studies, such as T-tubules [18], caveolae [19], or intercalated discs [20]. Despite the lack of molecular identification, there are several prominent candidates for mammalian cardiac SACs. Genetic screens in *Saccharomyces cerevisiae*, *Caenorhabditis elegans*, *Drosophilia* and *Danio rerio* indicated that transient receptor potential (TRP) channels subunits are involved in mechanical sensing [21, 22, 23]. The TRP channels form a large family of cationic channels that likely function as tetramers in various processes and have been recently recognized as key molecules in pathological cardiac hypertrophy and heart failure [24, 25].

Canonical TRP channels (TRPCs) are a group of mammalian Ca^{2+}-permeable channels which mediate store-operated Ca^{2+} entry as well as store-independent Ca^{2+} influx [26, 27, 28]. TRPC1 channels are widely expressed in cardiac myocytes and may be located in T-tubules [18] which are consistent with the hypothesized spatial distribution of endogenous

SAC_{ns} [18]. In dystrophic fibers, TRPC1 have been involved in abnormal Ca^{2+} influx [29] and Ward *et al* [30] have shown that expression level of TRPC1 was increased in aged *mdx*-DCM heart. Studies in heterologous system demonstrated that TRPC1 expression induced a 10-fold increase of SAC_{ns} currents and TRPC1 inhibition through RNA antisens reduced these currents [31]. Subsequently, it has been shown that the specific SAC_{ns} blocker, GsMTx-4, blocked the expressed channel [32]. However, it has also been shown that GsMTx-4 could inhibit SACs formed probably with TRPC6 in smooth muscle [33]. TRPC6 is highly expressed in human heart homogenates [34]. This channel seems also to be located in T-tubules and can be translocated to the plasma membrane after stimulation with α_1-agonists [35]. Furthermore TRPC6 has been involved in the SAC_{ns} in ventricular cells because the current could be blocked by a TRPC6 antibody [36]. Thus both TRPC1 and TRPC6 are good candidates for mammalian SAC_{ns}.

TPRV2 channels have also been involved in the stretch-dependent responses in different cell types as murine aortic myocytes or cardiomyocytes [37, 38, 39]. In a physiological context, these channels have been shown to be involved in the formation and integrity maintenance of intercalated discs and in the mechanotransduction in these particular areas [20]. Moreover, Rubinstein *et al* [40] have demonstrated that TRPV2 channels could participate to the molecular mechanisms of increased cardiomyocyte contractility. Indeed, authors have suggested that these channels may participate to the sarcoplasmic reticulum (SR) Ca^{2+} load by a small local influx of Ca^{2+} in the vinicity of RyRs. Taking account these results, TRPV2 channels seem to be a good candidate for SAC_{ns}. In a pathological context, they have been demonstrated to be involved in the pathogenesis of myocyte degeneration in dystrophic muscle [41]. Their sarcolemmal accumulation has been shown in dystrophic ventricular cardiomyocytes in several studies [38, 39] suggesting a role in Ca^{2+} dysregulation which can lead to cardiomyocytes death.

Studying SACs is not trivial because of the need of technical skills and experience. Several methods have been developed to perform a mechanical stimulation including the use of glass microneedles [42], suction micropipettes [43] or adhesives [44]. Furthermore, others studies used cell swelling through hypoosmotic shock to investigate SACs activities in dystrophin deficient cardiomyocytes [45, 39]. This last technique leads to cell swelling through water entry needed to the equilibration of ionic gradients between the extracellular medium and cytosolic compartment. The consequent increase of cell volume can provide a three-dimensional stretch of the cell, but changes in volume are not easily related to changes in tension. In the literature, authors agree that it is difficult to distinguish between the effects of the stretch component and other possible effects of swelling, i.e. the changes in electrophysiology can't be compared with those due to homogenous or local stretch [46].

In this work, ventricular cardiomyocytes have been stretched using the carbon microfibers technique [47, 48] which has the advantage to achieve an almost homogenous lengthening of the sarcomeres and to best mimic the effect of diastolic filling in physiological conditions [49]. The effects of an axial stretch on cationic influx and on variations of intracellular calcium concentration ($[Ca^{2+}]_i$) were investigated in dystrophin-deficient ventricular cardiomyocytes. Moreover, with specific blockers, the involvement of TRPs channels in the observed Ca^{2+} influxes and intracellular concentration variations was explored.

2. Materials and methods

2.1. Cell isolation

The investigation was conducted in agreement with European Community Council directives as well as with the Guide for the Care and Use of Laboratory Animals published by the US National Institutes of Health (NIH Publication No.85-23, revised 1996).

Ventricular cardiac myocytes were isolated from 10 to 12 months male C57BL10Scsn (WT) mice and C57/BL10ScScn-*mdx* mice (Jackson Laboratory). Mice were euthanized by cervical dislocation, followed by rapid removal of the heart and subsequent enzymatic dissociation of the left ventricular tissue as previously described [50].

2.2. Solutions and chemicals

Before experiments, cells were stored in culture medium containing Dulbecco's modified Eagle's medium (DMEM – Lonza), complemented with 10 µg/mL insulin, 10 µg/mL gentamycin, 4 mM $NaHCO_3$, 10 mM Hepes, 0.2 % BSA and 12.5 µM blebbistatin (all from Sigma). During experiments, cardiomyocytes were superfused with Tyrode solution containing 140 mM NaCl, 5.4 mM KCl, 1.8 mM $CaCl_2$, 1.8 mM $MgCl_2$, 10 mM Hepes and 11 mM glucose or with calcium-free Tyrode solution containing 140 mM NaCl, 5.4 mM KCl, 1.8 mM $MgCl_2$, 10 mM Hepes, 11 mM glucose, 1 g/L BSA and 20 mM Taurine.

Tranilast (Trn) was purchased from Calbiochem, GsMTx-4 from Abcam , probenecid (Prb), Streptomycin sulfate (Strp) and 4-methyl-4'-[3.5-bis(trifluoromethyl)-1H-pyrazol-1-yl]-1.2.3-thiadiazole-5-carboxanilide (YM-58483) from Sigma, ryanodine from Merck, fura-2-AM and fluo-8-AM from Santa-Cruz .

2.3. Mechanical stimulation

Axial stretch of single myocyte was performed with the micro-carbon fibers technique previously described [49, 48]. Briefly, a pair of carbon fibers (40 µm diameter, GRC-Graphite-reinforced carbon - TMIL - *Tsukuba Materials information Laboratory, Ltd,* Tsukuba, Japan) was mounted in glass capillaries, whose thin ends were bent by 30° to ensure near-planar approach of carbon fibers to the cell surface. One carbon fiber each was attached to

either end of a cardiomyocyte (fig. 1 A), using separate three-axis miniature hydraulic manipulators. Axial stretch was performed through the lateral movement of fiber and sarcomere length was measured with a high speed camera and dedicated software (Sarclength, Ionoptix) by means of a FTT procedure.

2.4. Intracellular calcium measurements using confocal microscopy

Cells were loaded at room temperature during 20 min with the single-wavelength calcium sensitive probe fluo-8-AM (6 µM) in Ca^{2+}-free Tyrode solution. Cells were stretched at 10 % of the initial sarcomere length before recording fluorescence.
Fluorescence images were recorded by Confocal Laser Scanning Microscopy (CLSM) using a Bio-Rad MRC 1024 (Bio-Rad Laboratories) equipped with a 15 mW Ar-Kr gas laser. Confocal unit was attached to an inverted microscope (Olympus IX70) with a 60X water objective and fluorescence signal collection was performed through the control software Lasersharp 3.2 (Bio-Rad Laboratories). Fluorophore was excited with 488 nm line and the emitted fluorescence was detected at 522 nm (green fluorescence). For analysis, fluorescence was normalized (DF/F_0) and calculated through IDL software routines [51].

2.5. Mn^{2+}-quenching experiments

Cardiomyocytes were incubated for 45 min at 37°C, 5 % CO_2 in culture medium with 3 µM (final concentration) of fura-2-AM probe. After being loaded, cells were washed with Ca^{2+}-free Tyrode solution before measurement of cation influx. Fura-2 loaded cells were excited at 360 nm with a CAIRN monochromator (Cairn Research Limited, Faversham, UK), and emission fluorescence was monitored at 510 nm using a CCD camera (Photonic Science, Robertsbridge, UK) coupled to an Olympus IX70 inverted microscope (60X water immersion fluorescence objective). The influx of Mn^{2+} through cationic channels was evaluated by the quenching of the fura-2 fluorescence excited at 360 nm, i.e., at the isosbestic point. The variation of fluorescence was recorded through the Imaging Workbench 4.0 (IW 4.0) software (Indec BioSystems, Mountain View, CA). The rate of fluorescence intensity loss at 360 nm was divided by the initial fluorescence intensity in the cell measured before the addition of manganese ions to correct for differences in the cell size or fura-2 loading. The maximal rate of quench of the fluorescence intensity, expressed as percent per minute, was obtained using a linear regression analysis.

2.6. Statistical analysis

Data are presented as means ± SEM, n is the number of cells. Differences were tested with *t*-test. $P < 0.05$ indicates a statistical significant difference.

3. Results

3.1. Cationic influxes and $[Ca^{2+}]_i$ increases in axial stretch condition

Ventricular cardiomyocytes have been stretched using the carbon microfibers technique (Fig.1) Two carbon fibers were connected to micromanipulators (3 axis) allowing to gently move each fiber. In this protocol, one fiber served as an anchor with no movement during the experiment time (CF1 in Fig.1 A and B). Axial stretch was carried out through lateral movement of the other fiber (CF2 in Fig.1 A and B) and the length of stretch was graded to cause an increase of sarcomere length of ≈ 10 %. In all experiments, a high speed camera associated to the Sarclength software allowed us to measure and check the sarcomere length (Fig. 1 B: inset).

Fig. 1 C illustrates the quenching of fura-2 fluorescence in cardiomyocytes in response to Mn^{2+} perfusion. Mn^{2+} ions are assumed to enter the cell through the same pathways as the ones used by Ca^{2+}, and once within the cells, these ions are trapped in the cytosol and strongly quench the fluorescence emitted by the fura-2 Ca^{2+} dye. In resting (no stretch) WT cardiomyocytes, no significant variation of fura-2 fluorescence intensity was observed after Mn^{2+} perfusion. However, maintaining WT cardiomyocytes in stretching conditions generated an important decrease of the fura-2 fluorescence. Interestingly, in resting *mdx* cardiomyocytes, a decrease of the fluorescence intensity was observed after the perfusion of Mn^{2+} suggesting the presence of a constitutive cationic entry in this condition. This decrease was further enhanced in stretched *mdx*, higher than in stretched WT cardiomyocytes. In similar stretching conditions (Fig. 1 D), intracellular Ca^{2+} concentration ($[Ca^{2+}]_i$) was measured using the Ca^{2+} dye fluo-8 and using a perfusion protocol starting initially with a calcium free Tyrode solution followed by the perfusion of 1.8 mM Ca^{2+} Tyrode solution. In these conditions, $[Ca^{2+}]_i$ was not changed in resting WT cardiomyocytes whereas it was significantly increased during stretch. In resting *mdx*, the extracellular Ca^{2+} solution induced an increase of the fluo-8 fluorescence and in stretching conditions, *mdx* cardiomyocytes displayed a strong increase of fluo-8 fluorescence intensity. These results demonstrate that axial stretch allows both sarcolemmal influxes and increases of $[Ca^{2+}]_i$ in WT and *mdx* cardiomyocytes. Moreover, the delay from the perfusion to the $[Ca^{2+}]_i$ maximal increase was longer in WT cardiomyocytes as compared to *mdx* cells. This result shows a faster stretch-dependent calcium response in *mdx* cardiomyocytes as compared to WT.

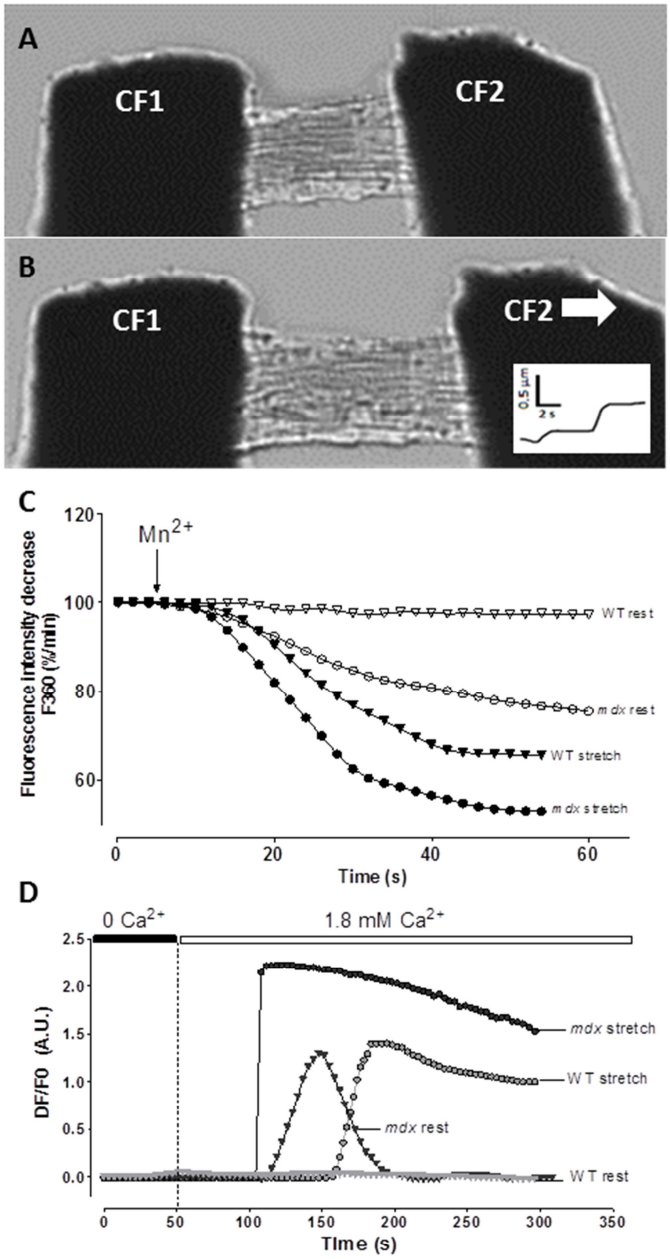

Figure 1

Figure 1: Representative stretch-dependent calcium responses in WT and *mdx* cardiomyocytes. A: resting cardiomyocyte attached to two carbon fibers (CF). B: gradually increase of the sarcomere length by micromanipulator-induced movement of one of CF. C: representative recordings of fura-2 fluorescence during perfusion with 300 µM Mn^{2+} obtained in resting WT (open triangles) and *mdx* (open circles) cardiomyocytes and in stretched WT (black triangles) and *mdx* (black circles). D: representative recordings relative of fluo-8 fluorescence in resting WT (grey triangles) and *mdx* (black triangles) and in stretched WT (grey circles) and mdx (black circles) during a protocol perfusion starting.

3.2. Involvement of SACs in stretch-dependent cations influxes and $[Ca^{2+}]_i$ increases

In order to investigate which channels are involved in cation entry and $[Ca^{2+}]_i$ increases observed in our experiments, inhibitors of SACs, L-type Ca^{2+} channels and ryanodine receptors (RyRs) have been used (Fig.2). Bars in Fig.2 A represent cations entry at rest and in stretched WT and *mdx* cardiomyocytes measured as means slope of fura-2 fluorescence intensity decrease (in %/min). It has to be noticed that stretching conditions showed higher cationic entries as compared to resting conditions in both WT (25 ± 3 %/min (*n=14),* white bars *and* 1.4 ± 0.5 %/min (n=19), clear grey declined hatching, respectively) and *mdx* cardiomyocytes (49 ± 7 %/min (*n=14*), white bars *and* 10.3 ± 1.5 %/min (n=12), clear grey declined hatching, respectively). Concerning stretch, first, in control conditions (white bars) stretched *mdx* cardiomyocytes showed a higher cationic entry as compared to stretched WT (49 ± 7 %/min (*n=14*) and 25 ± 3 %/min (*n=14*) respectively). Second, cardiomyocytes have been incubated in the presence of SACs blockers to assess their involvement in the stretch-dependent cationic influx. The aminoglycoside antibiotic streptomycin (Strp) has been reported to be a non-specific inhibitor for SACs and to reduce Ca^{2+} leak influx in resting muscle [30]. In WT cardiomyocytes, incubation with 300 µM Strp strongly inhibited stretch-dependent cation influx to 1.6 ± 0.7 %/min (*n=13*) (grey bar) whereas in *mdx* cardiomyocytes, incubation with Strp only partly blocked this influx to 10 ± 3 %/min (*n=12*). The most specific inhibitor for SACs available today is the tarantula spider toxin GsMTx-4 [52, 53]. Likewise, in WT cardiomyocytes, incubation with 2.5 µM GsMtx-4 (black bars) reduced the fluorescence quenching rate to 6 ± 1 %/min (*n=5*) whereas in *mdx* cardiomyocytes, GsMTx-4 incubation reduced stretch-dependent cation influx to 26 ± 1 %/min (*n=4*). In addition, the possible involvement of L-type Ca^{2+} channels has also been studied using nifedipine. In WT cardiomyocytes, incubation in 10 µM nifedifine (vertical hatching) did not lead to any inhibition of cation influxes (to 38 ± 3 %/min (*n=5*)) and led only to a weak reduction in *mdx* cardiomyocytes (24 ± 6 %/min (*n=6*)). Taken together, these results suggest that stretch-dependent cation influxes are partly due to SACs rather than L-type Ca^{2+} channels.

In the same stretching conditions, increase of $[Ca^{2+}]_i$ have been investigated (Fig. 2 B) reached during superfusion of calcium containing Tyrode solution in WT and *mdx* cardiomyocytes in control and in presence of SACs blockers. It has to be also noticed that stretching conditions showed higher $[Ca^{2+}]_i$ increase as compared to resting conditions in both WT (1.5 ± 0.2 a.u. (*n=10*), white bars *and* 0.30 ± 0.04 a.u.(n=12), clear grey declined hatching, respectively) and *mdx* cardiomyocytes (2.4 ± 0.1 a.u. (*n=12*), white bars *and* 1.38 ± 0.01 a.u. (n=12), clear grey declined hatching, respectively). As results obtained for cation influxes, in control conditions, stretched *mdx* cardiomyocytes displayed a higher increase of the $[Ca^{2+}]_i$ peak amplitude (2.4 ± 0.1 a.u. (*n=12*)) as compared to WT (1.5 ± 0.2 a.u. (*n=10*)

white bars). In WT cardiomyocytes, incubation with 300 µM Strp strongly decreased the $[Ca^{2+}]_i$ peak amplitude (0.20 ± 0.06 a.u. (*n=7*) grey bar), whereas in *mdx* cardiomyocytes, Strp incubation only reduced partly the stretch-dependent $[Ca^{2+}]_i$ response (1.47 ± 0.20 a.u. (*n=6*)). In WT cells, incubation with GsMTx-4 did not significantly modify the maximal amplitude of $[Ca^{2+}]_i$ response (1.90 ± 0.40 a.u. (*n=5*) dark bar) whereas in *mdx* cardiomyocytes GsMTx-4 incubation reduced the $[Ca^{2+}]_i$ increase (1.07 ± 0.17 a.u. (*n=5*)). Channels involved in the excitation-contraction (EC) coupling have also been studied on the increase of $[Ca^{2+}]_i$. In WT cardiomyocytes, incubation with 10 µM nifedipine strongly blocked stretch-dependent $[Ca^{2+}]_i$ increase (0.39 ± 0.12 a.u. (*n=5*), vertical hatching) while in *mdx* cardiomyocytes, nifedipine incubation did not significantly change the $[Ca^{2+}]_i$ response (1.94 ± 0.30 a.u. (*n=5*)). Incubation with 100 µM ryanodine, able to block ryanodine receptors, induced a strong decrease of $[Ca^{2+}]_i$ response both in WT cardiomyocytes (0.48 ± 0.43 a.u.(*n=9*) declined hatching) and in *mdx* cells, (0.55 ± 0.30 a.u. (*n=7*)) declined hatching).

These results suggest that stretch-dependent cationic influxes are strongly inhibited by SACs blockers in WT cardiomyocytes. However, inhibition of SACs was observed to be only partial in *mdx* cardiomyocytes. In addition, even if excitation-contraction coupling activation seemed not involved in these influxes, the observed $[Ca^{2+}]_i$ responses appear to strongly depend on ryanodine receptors.

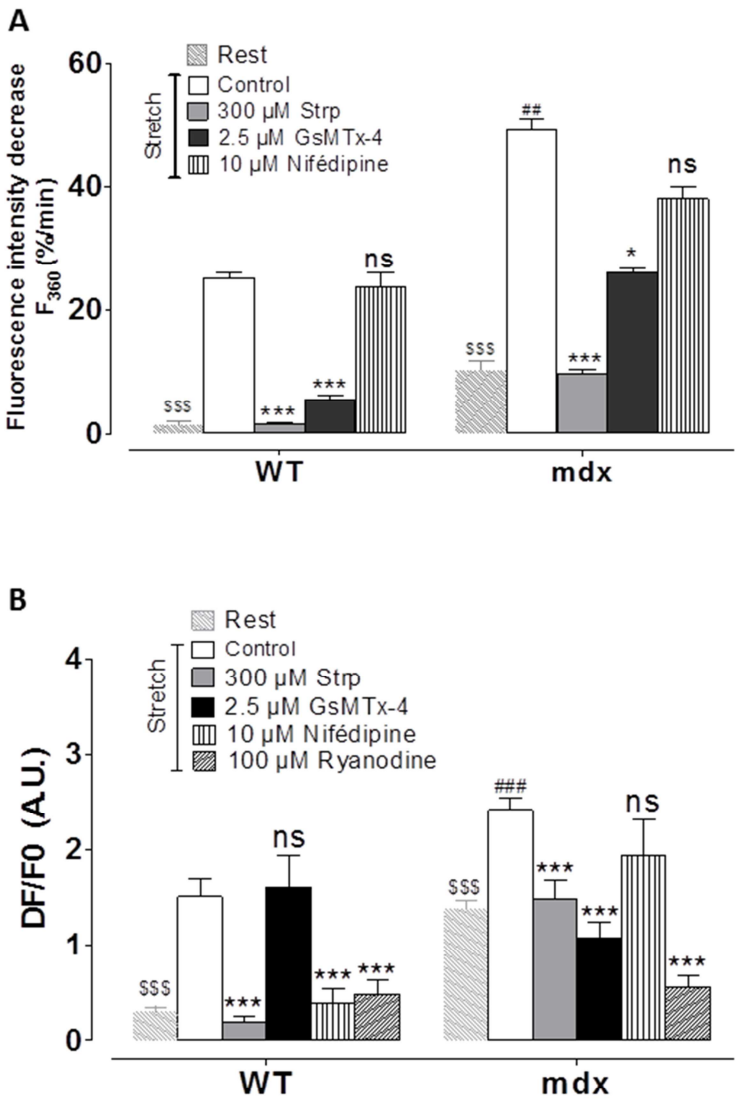

Figure 2

Figure 2: Effects of SACs blockers and blockers of EC coupling actors on stretch-dependent responses. Cells were incubated with 300 µM streptomycin (Strp, grey bars) or 2.5 µM GsMTx-4 (Black bars) for SACs inhibition and with 10 µM nifedipine (vertical hatching) or 100 µM ryanodine (declined hatching) for EC coupling inhibition. Open bars represent the control. A: Mn^{2+} influx in WT and *mdx* cardiomyocytes maintained in stretched condition. Measurements are represented as slopes of the Mn^{2+}-induced decreasing phase of fura-2 fluorescence measured at 360 nm and expressed as percent decrease per minute. Bar-graphs represent mean rates of fluorescence decrease induced by Mn^{2+} (expressed at % /min) ± SEM. B: maximal amplitude of fluo-8 fluorescence intensity in WT and *mdx* cardiomyocytes maintained in stretched condition. Measurements are represented as mean normalized fluo 8 fluorescence intensity ± SEM. * P<0.01; *** P<0.001; ns, not significant. ## represents the statistical difference between WT and *mdx* in stretched conditions. ## $p < 0.005$; ### $p < 0.001$. $$$ represents the statistical difference between resting and stretched conditions. $$$ $p < 0.001$.

3.3. Involvement of TRPV2 channels in stretch-dependent cations influxes and $[Ca^{2+}]_i$ increases

Because TRPV2 channels have been identified as molecular candidates for stretch-activated channels [37, 54] their involvement have been investigated in our *mdx*-DCM model (Fig. 3). Fig. 3 A illustrates the quenching of fura-2 fluorescence in stretched cardiomyocytes in response to Mn^{2+} perfusion in the presence of an antibody raised against an extracellular epitope of the channel (AB TRPV2 extra). If the channel pores are indeed blocked by this antibody, this strategy suppresses the TRPV2 protein function. In WT cardiomyocytes (triangles), incubation with AB TRPV2 extra (filled triangles) did not modify fura-2 fluorescence intensity decrease during perfusion of Mn^{2+} whereas in *mdx* cardiomyocytes (circles), AB TRPV2 extra incubation (open circles) led to a strong inhibition.

Taking into account this result, immunostaining of TRPV2 channels has been performed with anti-TRPV2 antibody (Fig 3. B) and a strong difference of TRPV2 localization was observed between WT and *mdx*. In WT cardiomyocytes, TRPV2 immunostaining revealed sarcolemmal and intracellular localizations of this protein. By contrast *mdx* cardiomyocytes displayed only a significant TRPV2 localization at the sarcolemma. Fluorescence profiles drawn at the yellow line position evidenced the sarcolemmal localizations of TRPV2 *mdx* cardiomyocytes. To quantify the expression of the TRPV2 protein, western blot has been performed in mdx and WT cardiomyocytes. Fig. 3 C shows an example (left panel of Fig. 3 C) western blots obtained from isolated ventricular WT and *mdx* cardiomyocytes, and TRPV2 expression was shown relative to actin expression. No drastic difference was found in the whole expression levels of TRPV2 in WT and *mdx*. Nevertheless, a two bands (A and B) profile, possibly corresponding to two different TRPV2 maturation forms, was observed, and particularly in *mdx* blots. Distribution of the two bands (Fig. 3 C) has been analyzed. The ratio A/B showed (right panel of Fig. 3 C) a different distribution between WT and *mdx*. Indeed, band A was more represented in WT cardiomyocytes (A/B = 1.44 ± 0.07 (*n=4*)). In *mdx* cardiomyocytes, band B was found equivalent to band A (0.95 ± 0.13 (*n=4*)). These results suggest different post-translational maturation of the TRPV2 protein in WT and *mdx* cells. These findings clearly indicate differences in both localization and maturation between WT and *mdx* cardiomyocytes that probably can lead to the modification of TRPV2 function.

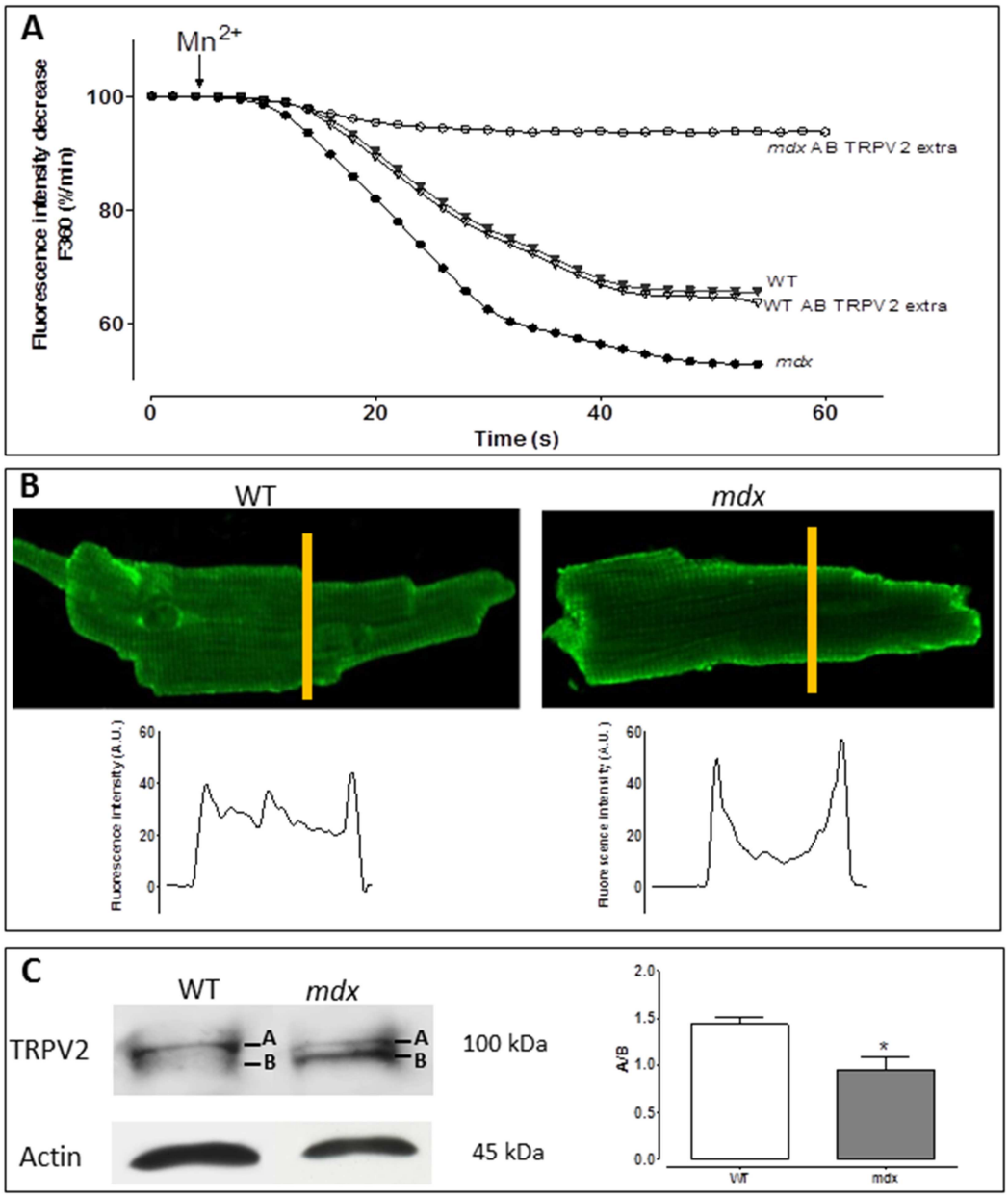

Figure 3

Figure 3: Study of TRPV2 channels: A: example of recordings of fura-2 fluorescence during perfusion with 300 µM Mn^{2+} obtained from stretched WT (black triangles) and stretched *mdx* (black circles) and after incubation with AB TRPV2 extra from stretched WT (open triangles) and *mdx* (open circles) cardiomyocytes. B: example of immunostaining of TRPV2 channels and profile of the staining from WT (left panel) and *mdx* cardiomyocytes. Vertical yellow lines represent the location where profiles were computed. C: An example of Western blot lanes of TRPV2 channel (left). On the right, bar-graphs represents the mean ratio of band A over B *(n=4)*. *P<0.01.

3.4. Inhibition and activation of stretch-dependent responses with TRP modulators

Fig. 4 displays stretch-dependent cation influxes and $[Ca^{2+}]_i$ increases in the presence of three TRP inhibitors. Effects have been calculated as maximal slopes of the Mn^{2+}-induced decreasing phase of fura-2 fluorescence measured at 360 nm (F_{360}) and expressed as percent decrease per minute (Fig. 4 A). In WT cardiomyocytes, as it could be observed in Fig. 3 A, incubation with AB TRPV2 extra did not block the cationic influx (28 ± 7 %/min (*n=5*) dark grey bars) observed in control (25 ± 3 %/min (*n=14)* white bars) whereas in *mdx* cardiomyocytes, a strong inhibition could be observed (to 7 ± 2 %/min (*n=6*) in the presence of this antibody as compared to control (49 ± 7 %/min (*n=14*)). Similar effects could be observed with Tranilast (Trn), for which it has been reported a strong specificity for TRPV2 channels. In WT cells, incubation with 100 µM Trn did not significantly reduce the cationic influx (19 ± 4 %/min (*n=13*) light grey bar) as compared to control (25 ± 3 %/min). In *mdx* cardiomyocytes, Trn incubation drastically reduced the cationic influx (9 ± 2 %/min (*n=13*) as compared to 49 ± 7 %/min (*n=14*) in control). The application of 2 µM of YM-58483, a TRPCs blocker, induced a high inhibition of the cationic influx both in WT and mdx cardiomyocytes (5± 2 %/min (*n=10*) horizontal hatching, and 9 ± 3 %/min (*n=7*) respectively). Moreover, in *mdx* cardiomyocytes, incubation with 100 µM Trn and 2 µM YM almost completely blocked cationic influxes (data not shown). TRPs inhibitors effects have also been measured on stretch-dependent $[Ca^{2+}]_i$ increase. Fig. 4 B shows the effect of TRPV2 and TRPCs blockers on the peak amplitude of $[Ca^{2+}]_i$ increase. In WT cardiomyocytes, incubation with AB extra TRPV2 induced a small inhibition of the $[Ca^{2+}]_i$ increase (to 0.97 ± 0.25 a.u. (*n=6*) (dark grey bars) as compared to control (white bars 1.5 ± 0.2 a.u. (*n=10*)). In *mdx* cardiomyocytes, incubation with AB extra TRPV2 reduced the $[Ca^{2+}]_i$ increase (1.56 ± 0.16 a.u. (*n=6*)) as compared to control (2.4 ± 0.1 a.u. (*n=12*)). Interestingly, in WT cardiomyocytes, incubation with 100 µM Trn induced a strong decrease of peak amplitude of $[Ca^{2+}]_i$ (0.19 ± 0.03 a.u. (*n=6*) (clear grey bars)) whereas in *mdx* cardiomyocytes, Trn incubation only induced a moderate decreased the stretch-dependent $[Ca^{2+}]_i$ increase (1.73 ± 0.14 a.u. (*n=7*)). In addition, in WT cells, 2 µM YM (an inhibitor of TRPCs channels) induced a decrease of the maximal amplitude of $[Ca^{2+}]_i$ (0.81 ± 0.11 a.u. (*n=8*)) in contrast with *mdx* cardiomyocytes where it did not significantly modify the $[Ca^{2+}]_i$ peak (2.49 ± 0.33 a.u. (*n=9*)).

To assess TRPV2 activity, another pharmacological approach (Fig. 5) has been applied with the use of probenecid (Prb), a TRPV2 activator [40]. In WT cells, incubation with 1 nM of Prb (Fig. 5 A) induced a significant increase of cationic influxes (to 39 ± 12 %/min (*n=7*) black bars) as compared to control condition (white bars, 25 ± 3 %/min). In contrast, in *mdx* cardiomyocytes, incubation with 1 nM Prb did not change the stretch-dependent cationic influx (43 ± 8 %/min (*n=7*)). Similarly, in WT cells, the use of 1 nM Prb (Fig. 5 B) induced a

significant increase of peak amplitude of $[Ca^{2+}]_i$ (2.6 ± 0.2 a.u. (*n=8*) black bars, control; 1.5 ± 0.2 a.u. (*n=10*)) but not in *mdx* cells (2.4 ± 0.2 a.u. (*n=8*), control: 2.4 ± 0.1 a.u. (*n=12*). Because, delays were observed in $[Ca^{2+}]_i$ increase, two kinetic parameters have been measured (Fig. 5 C and D). In WT cardiomyocytes, incubation with 1 nM Prb induced a significant decrease of the time to response onset (40 ± 6 s (*n = 11)*) as compared to control (97 ± 17 s (*n = 16*) (Fig. 5 C)). In *mdx* cell, probenecid incubation did not change this delay (35 ± 5 s (*n = 9*)) as compared to control (50 ± 7 s (*n = 14*)). Furthermore, in WT cardiomyocytes, incubation with 1 nM Prb led a significant decrease of the time to reach maximal amplitude (10 ± 1 s (*n = 11*)) as compared to control (40 ± 5 s (*n = 16*) (Fig. 5 D)) whereas in mdx cells, this parameter did not significantly change (12 ± 2 s (*n = 9*)) as compared to control (7 ± 2 s (*n = 14*)).

Taken together these findings suggest that stretch-dependent Ca^{2+} influxes and stretch-dependent Ca^{2+} increases depend, in WT cardiomyocytes, on TRP channels but not on TRPV2. In *mdx* cardiomyocytes, these stretch-dependent Ca^{2+} responses depend both on TRPV2 and TRPCs channels, meaning that the TRPV2 channels could play a key role in the calcium dysregulation in *mdx* cardiomyocytes, enhanced in stretching conditions. The unability of probenecid to increase Ca^{2+} responses in *mdx* reveals that TRPV2 channels could be in an overactivated state in a dystrophin deficient context.

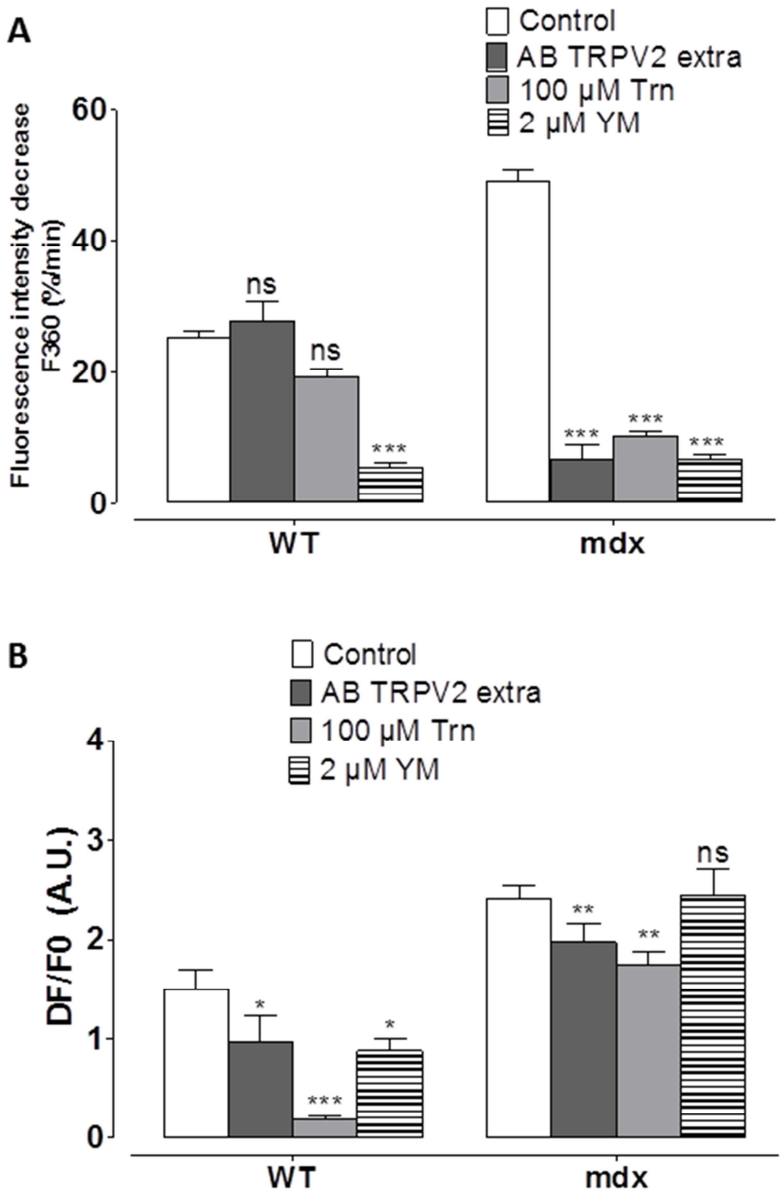

Figure 4

Figure 4: Effect of TRPs inhibitors in stretched cardiomyocytes. Cells were incubated with TRPs blockers: antibody against an extracellular epitope of TRPV2 (dark grey bars), 100µM tranilast (clear grey bars) and YM-48483, inhibitor of TRPCs channels in stretched WT and *mdx* cardiomyocytes. Open bars represent the control. A: Mn^{2+} influx in WT and *mdx* cardiomyocytes maintained in stretching condition. Measurements are represented as slopes of the Mn^{2+}-induced decreasing phase of fura-2 fluorescence measured at 360nm and expressed as percent decrease per minute. Bar-graphs represent mean rates of fluorescence decrease induced by Mn^{2+} (expressed at % /min) ± SEM. B: maximal amplitude of fluo 8 fluorescence in WT and *mdx* cardiomyocytes maintained in stretching condition. Measurements are represented as mean normalized fluo-8 fluorescence intensity ± SEM. * P<0.01; ** P<0.005; *** P<0.001; ns, no significant.

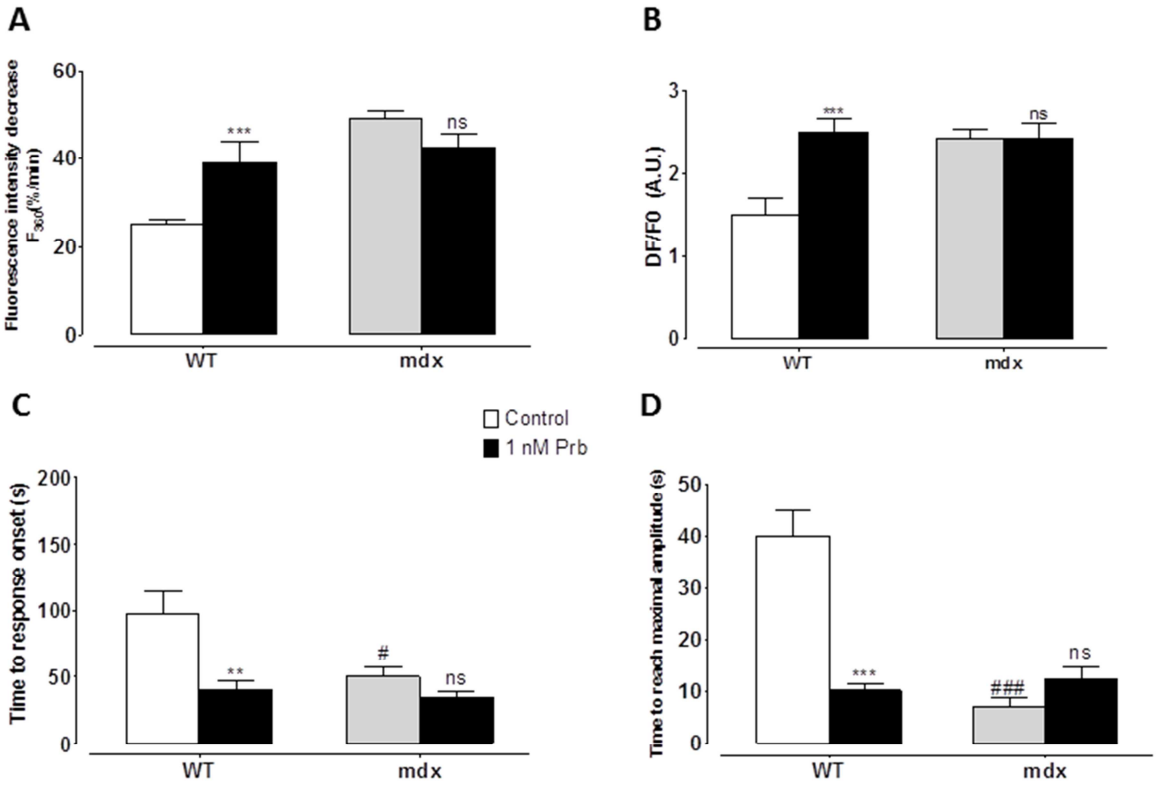

Figure 5

Figure 5: Effect of probenecid, a TRPV2 activator in stretched cardiomyocytes. Cells were incubated with 1nM probenecid (Prb, black bars). Open bars represent the control and clear grey bars *mdx* cardiomyocytes in resting condition. A: Mn^{2+} influx in WT and *mdx* cardiomyocytes maintained in stretching condition. Measurements are represented as slopes of the Mn^{2+}-induced decreasing phase of fura-2 fluorescence measured at 360nm and expressed as percent decrease per minute. Bar-graphs represent mean rates of fluorescence decrease induced by Mn^{2+} (expressed at % /min) ± SEM. B: maximal amplitude of fluo 8 fluorescence in WT and *mdx* cardiomyocytes maintained in stretching condition. Measurements are represented as mean normalized fluo-8 fluorescence intensity ± SEM. C: time between the beginning of the 1.8 mM Ca^{2+} perfusion and the start of the normalized fluo-8 fluorescence intensity increases. Measurements are represented as mean of the time to response onset (expressed in second) ± SEM. D: time between the start of the normalized fluo-8 fluorescence intensity increase and maximal amplitude. Measurements are represented as mean of the time to reach maximal amplitude of fluorescence signal (expressed in seconds) ± SEM. * P<0.01; *** P<0.001; ns, no significant. ## represents the statistical difference between WT and *mdx* in stretched conditions. # p < 0. 01; ### p < 0.001. ns, no significant.

4. Discussion

Using carbon microfibers technique, an axial stretch was applied to mimic effects of physiological conditions of the ventricular filling. Study on cation influxes by the Mn^{2+}-quenching technique demonstrated a high stretch-dependent cationic influx in dystrophic cells, partially due to SACs. Moreover, the variation of intracellular calcium concentration ($[Ca^{2+}]_i$) measured by fluorescence confocal imaging showed also a higher increase in *mdx* cardiomyocytes which depends on Ca^{2+} influx through SACs, enhanced by a Ca^{2+} induced Ca^{2+} release (CICR) mechanism. Involvement of TRPs channels in this excessive Ca^{2+} influx has been investigated using specific modulators and demonstrated both sarcolemma localization and an abnormal activity of TRPV2 channels.

4.1. Axial stretch-dependent influx and SACs

It is widely accepted that membrane of dystrophin-deficient cardiomyocytes is more fragile, making these cells more susceptible to mechanically induced damage. This loss of membrane integrity leads to an increase of permeability which allows an abnormal stress-induced influx of Ca^{2+}. The stretch-activated channels (SACs) have been proposed to mediate these abnormal Ca^{2+} entries in DMD skeletal muscle [15, 55] and in *mdx* cardiomyocytes [39, 45). Nevertheless, in these studies, the mechanical stress applied on cardiomyocytes was a hypoosmotic shock which triggers a cell swelling. In this condition, it is not sure if the same channels are involved in a physiological diastolic stretch. In this study, an homogenous axial stretch was carried out to mimic the effects of a diastolic stretch.

The present results show that an homogenous axial stretch can create conditions for the présence and/or the activation of cationic permeant sarcolemmal channels. The cationic influx observed in *mdx* cardiomyocytes is more important than in WT in agreement with the hypothesis of dysregulation of sarcolemmal channels. This observed cationic influx has been attributed, in part, to activation of the SACs. The evidence is based on the results obtained from a combination of two inhibitors: streptomycin, which is not only a blocker of SACs but can also modulate Ca^{2+} and K^+ channels in cardiac muscle [56, 57], and the most specific inhibitor of cationic non selective SACs known today, the tarentula toxin, GsMTX-4. These two SACs blockers lead to the cationic influx inhibition, although not completely. This later fact suggest that cationic influx pathways other than SACs are present as well.

It has been demonstrated that axial stretch can induce depolarization of the resting potential and prolongation of the action potential which can trigger after-depolarization and extrasystoles [58]. These results would suggest an increase of Ca^{2+} influx through L-type Ca^{2+} channels. Here, the use of nifedipine does not significantly modify the stretch-dependent cationic influx which excludes, in our conditions, the activation of these channels by axial stretch and the consecutive calcium entry through this way.

4.2. Involvement of SACs influx and CICR in stretch-dependent intracellular calcium increase

Abnormal high intracellular free calcium concentration ($[Ca^{2+}]_i$) is thought to be involved in the progressive degeneration of muscle cells in DMD. Here, sarcolemma cationic influx appears to be higher in *mdx* cardiomyocytes and is partly due to SACs. However, do these influxes are sufficient to increase the $[Ca^{2+}]_i$? Axially stretching cardiomyocytes bathing in an extracellular calcium containing solution (1.8 mM) has no effect on $[Ca^{2+}]_i$ (data not shown). As some works have demonstrated that extracellular Ca^{2+} can block the SACs in a fast and flickering manner even at physiological concentrations [58, 59], our experiments have been performed by initially bathing cells in a free-Ca^{2+} solution and then perfusing 1.8 mM Ca^{2+} solution. This perfusion allows to induce cation entry and could avoid the possible flickering inhibition of SACs by Ca^{2+} from the beginning of the experiment. At rest, perfusing extracellular 1.8 mM Ca^{2+} triggered an increase of $[Ca^{2+}]_i$ in *mdx* but not in WT cardiomyocytes. Regarding the cationic movements, these results are similar to those obtained with the quenching technique where a constitutive influx is observed only in *mdx* cardiomyocytes after perfusion of Mn^{2+}. Interestingly, it can be noted that this increase is delayed by several tens of secondes. This could be due to translocation events occuring after a Ca^{2+} signal. In stretching conditions, our results support the hypothesis of an excessive calcium entry in *mdx* cardiomyocytes as the application of SACs blockers reduced the $[Ca^{2+}]_i$. The involvement of another source of Ca^{2+} has been proposed to be involved in damaged dystrophic muscle like an abnormal activation of the calcium induced calcium release (CICR) signalling pathway which has been demonstrated to contribute to the amplification in Ca^{2+} signal [60]. In our experiments, inhibition with high concentration of ryanodine reduced the stretch-dependent calcium increase in *mdx* cardiomyocytes. Nevertheless, L-type calcium channels which trigger the CICR are not normaly activated by membrane stretch, suggesting that Ca^{2+} entry through sarcolemmal channels could increase $[Ca^{2+}]_i$ and also stimulate the CICR mechanism leading to an amplification process. In WT cardiomyocytes, the mechanism of stretch-dependent calcium increase seems to be different. Indeed, SACs inhibition did not decrease the Ca^{2+} signal, suggesting that the influx through SACs seems to be too small to increase alone the $[Ca^{2+}]_i$ but could be sufficient to induce CICR because high concentration of ryanodine significantly reduced the Ca^{2+} signal. Surprisingly, incubation with nifedipine induced a strong inhibition of the $[Ca^{2+}]_i$ increase whereas L-type channels are not involved in the cationic influx during an axial stretch. But, it have been demonstrate by Copello *et al* [61] that nifedipine can modulate on its own the sparks frequency, independently of Ca^{2+} entry. They have shown that nifedipine decreased

the sparks frequency, without direct effects on RyR2 channels or the sarco(endo)plasmic reticulum Ca^{2+}-ATPase (SERCA).

4.3. TRPV2 channel: a likely SACs candidate *in mdx* cardiomyocytes

In the present study, a stretch-dependent influx which could increase the $[Ca^{2+}]_i$ has been demonstrated. This sarcolemma influx seems to be mediated partly by SACs. The molecular identity for SACs involved in muscular dystrophy is unknown. However, some studies have proposed several candidates as potential SACs in *mdx* cardiomyocytes such as TRPV2 channels. Recently, a number of studies involved these channels in a pathological context of heart disease but are also focused on their physiological role. Indeed, TRPV2 channels seem to be involved in the formation and the maintenance of integrity of intercalated disks and have a key role in the mechanotransduction in these specific areas of cardiomyocytes [20]. In DMD, TRPV2 channels have been involved in the progression of the pathology in both skeletal and cardiac muscle with a abnormal sarcolemmal localization [38, 39]. Here, a sarcolemmal accumulation has also been observed in aged *mdx* cardiomyocytes, and in WT the localization is more intracellular. Moreover, a different profile of TRPV2 protein maturation has been observed between WT and *mdx* cardiomyocytes. This result suggests a different type of maturation that could lead to a different localization in the cell. To assess the function of these channels in our model different pharmacological tools have been used. First, inhibition of TRPV2 channels with application of a blocking antibody raised against an extracellular epitope of these channels (AB TRPV2 extra) strongly reduced the stretch-dependent cationic influx in *mdx* but not in WT cardiomyocytes. This could be related to the sarcolemmal localization in *mdx* cells. Second, an another, less specific, blocker of TRPV2 channels, tranilast, confirmed the data previously obtained with AB TRPV2 extra. Third, the use of probenicid, an activator of TRPV2 activity, induced an increase of the cationic influx during an axial stretch in WT but not in *mdx* cardiomyocytes. This suggest that TRPV2 channels could be already activated and an important involvement of TRPV2 channels in cationic entries in stretched *mdx*. Recents works have shown that TRPV2 channels are involved, in a physiological context and indirectly, in the EC coupling [40, 62]. Indeed, authors suggest that TRPV2 channels may participate in the Ca^{2+} handling machinery and contribute to normal baseline function. Interestingly, incubation with the two blockers of TRPV2 channels induced a reduction of $[Ca^{2+}]_i$ in WT cardiomyocytes with a strong effect of tranilast. These results support an involvement of TRPV2 channels in CICR. The hypothesis would be that these channels could be translocated from the intracellular compartment to plasma membrane and being activated in a secondary step. Moreover, the use of probenecid revealed also an involvement of TRPV2 channels in the increase of $[Ca^{2+}]_i$. Koch *et al* [62], have studied the effect of probenecid on WT cardiomyocytes in resting conditions and have

observed that incubation with probenecid gradually increased the $[Ca^{2+}]_i$, without Ca^{2+} influx. It was suggested that these channels could have an indirect role in sarcoplasmic reticulum loading. Indeed, these channels could induce a small local increase of Ca^{2+} concentration that could activate SR Ca^{2+} release. In *mdx* cardiomyocytes TRPV2 channels may be involved in the stretch-dependent cation influx and CICR seems to be stimulated by influx through SACs. Incubation with the two TRPV2 blockers revealed a reduction of the $[Ca^{2+}]_i$, and activation with probenecid did not show significant difference in the stretch-dependent calcium increase. This result is in agreement with the idea that the stretch-dependent cationic influx is not modulated by probenecid. The combinaison of the three molecules targeting TRPV2 channels allows to reinforce the hypothesis of TRPV2 channels involvement in the mechanical response in *mdx* but not in WT cardiomyocytes.

4.4. TPRCs channels: nice SACs candidate in WT cardiomyocytes

Finally the other molecular candidates for SACs, the TRPCs channels have been tested. Studies about TRPCs mechanosensitivity are controversial because of the lack of specific tools and most of the studies have been performed in heterologous systems. Moreover, because a direct mechanosensitivity of these channels has not been clearly prooved, the recent idea is that the stretch sensitivity could be indirect and needed one or more others components [23]. Nevertheless, it has been demonstrated that TRPC1 expression level was increased in patholological context of DMD [30] and RNA antisens of TRPC1 channels in skeletal myoblasts could reduce SACs activity [29]. TRPC6 channels have also been identified as SACs in a study where I_{SAC} was inhibited by pore blocking antibodies [35]. In our experiments, the stretch-dependent cationic influx seemed to be partly due to TRPCs channels because the use of the non-specific blocker of TRPCs channels, YM-58483, induced a strong inhibition in both WT and *mdx* cardiomyocytes. The effect of TRPCs inhibition reduced the $[Ca^{2+}]_i$ in WT cardiomyocytes. Increase of $[Ca^{2+}]_i$ was thought to be due to stimulation of CICR by influx through SACs. In this condition, TRPCs channels could be the molecular actor of this stimulation. In *mdx* cardiomyocytes, inhibition by YM did not significantly modify the $[Ca^{2+}]_i$, even if an inhibition of the influx through these channels has been observed. We can speculate that influx by TRPCs channels are not the primary pathway to modulate the $[Ca^{2+}]_i$ in our conditions.

Thus, in this study, aged dystrophin-deficient cardiomyocytes respond to a mechanical challenge differently from WT cells. Indeed, our results support the involvement of different type of channels involved in the stretch-dependent response with an abnormal cationic influx which could induce by it's own an increase of the intracellular calcium concentration. TRPV2 channels are demonstrated here to play a key role in Ca^{2+} influxes and dysregulation in

stretched dystrophin deficient cardiomyocytes. Thus, the function and the translocation pathway of TRPV2 channels could be relevant targets for pharmacological therapy of DMD pathology.

Conflict of interest

None declared.

Acknowledgments

This work was supported by grants (#16791) from the Association Française contre les Myopathies.

Reference List

[1] Ferlini A, Sewry C, Melis MA, Mateddu A and Muntoni F. X-linked dilated cardiomyopathy and the dystrophin gene. *Neuromuscul Disord*. 9 (1999) 339-346.

[2] Spurney CF. Cardiomyopathy of Duchenne muscular dystrophy: current understanding and future directions. *Muscle nerve*. 44 (2011) 8-19.

[3] Monaco AP, Bertelson CJ, Middlesworth W, Coletti CA, Aldridge J, Fischbeck *et al*. Detection of deletions spanning the Duchenne muscular dystrophy locus using a tightly linked DNA segment. *Nature*. 316 (1985) 842-845.

[4] Lorin C, Gueffier M, Bois P, Faivre JF, Cognard C and Sebille S. Ultrastructural and functional alterations of EC coupling elements in *mdx* cardiomyocytes: an analysis from membrane surface to depth. *Cell Biochem Biophys*. 66 (2013) 723-736.

[5] Sharpe KM, Premsukh MD and Townsend D. Alterations of dystrophin-associated glycoproteins in the heart lacking dystrophin or dystrophin and utrophin. *J Muscle Res Cell Motil*. 34 (2013) 395-405

[6] Gailly P. New aspects of calcium signaling in skeletal muscle cells: implications in Duchenne muscular dystrophy. *Biochem Biophys Acta*. 1600 (2002) 38-44.

[7] Petrof BJ, Shrager JB, Stedman HH, Kelly AM and Sweeney HL. Dystrophin protects the sarcolemma from stresses developed during muscle contraction. *Proc Natl Acad Sci U S A.* 90 (1993) 3710-3714.

[8] Lawler JM. Exacerbation of pathology by oxidative stress in respiratory and locomotor muscles with Duchenne muscular dystrophy. *J Physiol*. 589 (2011) 2161-2170.

[9] Whitehead NP, Streamer M, Lusambili LI, Sachs F and Allen DG. Streptomycin reduces stretch-induced membrane permeability in muscles from *mdx* mice. *Neuromuscul Disord*. 16 (2006) 845-854.

[10] Hopf FW, Turner PR and Steinhard RA. Calcium misregulation and the pathogenesis of muscular dystrophy. *Subcell Biochem*. 45 (2007) 429-464.

[11] Millay DP, Goonasekera SA, Sargent MA, Aronow BJ and Molkentin JD. Calcium influx is sufficient to induce muscular dystrophy through a TRPC-dependent mechanism. *Proc Natl Acad Sci U S A.* 106 (2009) 19023-19028.

[12] Alderton JM and Steinhard RA. How calcium influx through calcium leak channels is responsible for the elevated levels of calcium-dependent proteolysis in dystrophic myotubes. *Trends Cardiovasc Med*. 10 (2000) 268-272.

[13] Ruegg U, Nicolas-Métral V, Challet C, *et al*. Pharmalogical control of cellular calcium handling in dystrophic skeletal muscle. *Neuromuscul Disord*. 12 (2002) S155-S161.

[14] Reed A, Kohl P and Peyronnet R. Molecular candidates for cardiac stretch-activated ion channels. *Glob Cardiol Sci Pract*. 2 (2014) 9-25.

[15] Franco-Obregón A and Lansman JB. Changes in mechanosensitive channel gating following mechanical stimulation in skeletal muscle myotubes from the *mdx* mouse. *J Physiol*. 539 (2002) 391-407.

[16] Yeung EW, Whitehead NP, Suchyna TM, Gottlib PA, Sachs F and Allen DG. Effects of stretch-activated channel blockers on $[Ca^{2+}]_i$ and muscle damage in the *mdx* mouse. *J Physiol*. 562 (2005) 367-380.

[17] Williams IA and Allen DG. The role of reactive oxygen species in the hearts of dystrophin-deficient mdx mice. *Am J Physiol Heart Circ Physiol*. 293 (2007) H1969-H1977.

[18] Huang H, Wang W, Liu P, *et al*. TRPC1 expression and distribution in rat hearts. *Eur J Histochem: EJH*. 53 (2009) e26

[19] Kohl P and Ravens U. Cardiac mechano-electric feedback: past,present, and prospect. *Prog Biophys Mol Biol*. 82(2003) 3-9.

[20] Katanosaka Y, Iwasaki K, Ujihara Y, *et al*. TRPV2 is critical for the maintenance of cardiac structure and function in mice. *Nat Commun*. 5 (2014) 1-14.

[21] Colbert HA, Smith TL and Bargmann CL. OSM-9, a novel protein with structural similiraty to channels, is required for olfaction, mechanosensation, and olfactory adaptation in *Caenorhabditis elegans*. *J Neurosci*. 17 (1997) 8259-8269.

[22] Walker RG, Willingham AT and Zuker CS. A Drosophila mechanosensory transduction channel. *Science*. 287 (2000) 2229-2234.

[23] Patel A, Sharif-Naeini R, Folgering J, Bichet D, Duprat F and Honore E. Canonical TRP channels and mechanotransduction: from physiology to disease states. *Pflugers Arch*. 460 (2010) 571-581.

[24] Watanabe H, Murakami M, Ohba T, Ono K and Ito H. The pathological role of transient receptor potential channels in heart disease. *Circulation*. 73 (2009) 419-427.

[25] Eder P and Molkentin JD. TRPC channels as effector of cardiac hypertrophy. *Circ Res*. 108 (2011) 265-272.

[26] Minke B and Cook JA. TRP channel proteins and signal transduction. *Physiol Rev*. 82 (2002) 429-472.

[27] Nilius B. From TRPs to SOCs, CCEs, and CRACs: consensus and controversies. *Cell Calcium*. 33 (2003) 293-298.

[28] Kwan HY, Huang Y and Yao X. Regulation of canonical transient receptor potential isoform 3 (TRPC3) channel by protein kinase G. *Proc Natl Acad Sci U S A.* 101 (2004) 2625-2630.

[29] Vandebrouck C, Martin D, Colson-Van Schoor M, Debaix H and Gailly P. Involvement of TRPC in the abnormal calcium influx observed in dystrophic (*mdx*) mouse skeletal muscle fibers. *J Cell Biol*. 158 (2002) 1089-1096.

[30] Ward ML, Williams IA, Chu Y, Cooper PJ, Ju YK and Allen DG. Stretch-activated channels in the heart: contributions to length-dependence and to cardiomyopathy. *Prog Biophys Mol Biol*. 97 (2008) 232-249.

[31] Maroto R, Raso A, Wood TG, Kurosky A, Martinac B and Hamill OP. TRPC1 forms the stretch-activated cation channel in vertebrate cells. *Nat Cell Biol*. 7 (2005) 179-185.

[32] Bowman CL, Gottlib PA, Suchyna TM, Murphy YK and Sachs F. Mechanosensitive ion channels and the peptide inhibitor GsMTx-4: history, properties, mechanisms and pharmacology. *Toxicon*. 49 (2007) 249-270.

[33] Spassova MA, Hewavitharana T, Xu W, boloff J and Gill DL. A common mechanism underlies stretch activation and receptor activation of TRPC6 channels. *Proc Natl Acad Sci U S A.* 103 (2006) 16586-16591.

[34] Riccio A, Medhurst AD, Mattei C, *et al*. mRNA distribution analysis of human TRPC family in CNS and peripheral tissues. *Brain Res*. 109 (2002) 95-104.

[35] Dyachenko V, Husse B, Rueckschloss U and Isenberg G. Mechanical deformation of ventricular myocytes modulates both TRPC6 and Kir2.3 channels. *Cell Calcium*. 45 (2009) 38-54.

[36] Dyachenko V and Isenberg G. Ventricular myocytes: deformation induced sarcomere misalignment modulates TRPC6 and KIR2.3 channels. *In: Proceedings of the Fourth International Conference on Cardiac Mechano-Electric Feedback*. (2007).P.84

[37] Muraki K, Iwata Y, Katanosaka Y, *et al*. TRPV2 is a component of osmotically sensitive cation channels in murine aortic myocytes. *Circ Res*. 93 (2003) 829-838.

[38] Iwata Y, Ohtake H, Suzuki O, Matsuda J, Komamura K and Wakabayashi S. Blockade of sarcolemmal TRPV2 accumulation inhibits progression of dilated cardiomyopathy. *Cardiovasc Res*. 99(2013) 760-768.

[39] Lorin C, Vögeli I and Niggli E. Dystrophic cardiomyopathy - role of TRPV2 channels in stretch-induced cell damage. *Cardiovasc Res*. 106 (2015) 153-162.

[40] Rubinstein J, Lasko VM, Koch SE, *et al*. Novel role of transient receptor potential vanilloid 2 in the regulation of cardiac performance. *Am J Physiol Heart Circ Physiol*. 306 (2014) H574-H584.

[41] Iwata Y, Arai Y, Komamura K, Miyatake K and Shinohara M. A novel mechanism of myocyte degeneration involving the Ca^{2+}-permeable growth factor-regulated channel. *J Cell Biol.* 131 (2003) 957-967.

[42] Fabiato A. Myoplasmic free calcium concentration reached during the twitch of an intact isolated cardiac cell and during calcium-induced release of calcium from the sarcoplasmic reticulum of a skinned cardiac cell from the adult rat or rabbit ventricle. *J Gen Physiol*. 78 (1981) 457-497.

[43] Brady AJ. Mechanical properties of isolated cardiac myocytes. *Physiol Rev.* 71 (1991) 413-428.

[44] Prosser BL, Ward CW and Lederer JW. X-ROS signaling: rapid mechano-chemo transduction in heart. *Science*. 333 (2011) 1440-1445.

[45] Fanchaouy M, Polakova E, Jung C, Ogrodnik J, Shirokova N and Niggly E. Pathways of abnormal stress-induced Ca^{2+} influx into dystrophic *mdx* cardiomyocytes. *Cell Calcium*. 46 (2009) 114-121.

[46] Isenberg G, Kondratev D, Dyachenko V, Kazanski V and Gallitelli MF. Isolated cardiomyocytes: mechanosensitivity of action potential, membrane current and ion concentration. *Mechanosensitivity in Cells and Tissues.Moscow: Academia*. (2005)

[47] Le Guennec JY, Peineau N, Arbigay J, Mongo KG and Garnier D. A new method of attachment of isolated mammalian ventricular myocytes for tension recording: length dependence of passive and active tension. *J Mol Cell Cardiol*. 22 (1990) 1083-1093.

[48] Sugiera S, Nishimura S, Yasuda S, Hosoya Y and Katoh K. Carbon fiber technique for the investigation of single-cell mechanics in intact cardiac myocytes. *Nat protoc*. 1 (2006), 1453-1457.

[49] Yasuda SI, Sugiura S, Kobayawa N, *et al*,. A novel method to study contraction characteristics of a single cardiac myocyte using carbon fibers. *Am J Physiol Heart Circ Physiol*. 281 (2001) H1442-H1446.

[50] Kabaeva Z, Zhao M and Michele DE. Blebbistatin extends culture life of adult mouse cardiac myocytes and allows efficient and stable transgene expression. *Am J Physiol Heart Circ Physiol*. 294 (2008) H1667-H1674

[51] Mondin L, Balghi H, Constantin B, Cognard C and Sebille S. Negative modulation of inositol 1,4,5-trisphosphate type 1 receptor expression prevents dystrophin-deficient muscle cells death. *Am J Physiol Cell Physiol*. 297 (2009) C1133-C1145.

[52] Suchyna TM, Johnson JH, Hamer K, *et al*. Identification of a peptide toxin from Grammostola spatulata spider venom that blocks cation-selective stretch-activated channels. *J Gen Physiol*. 115 (2000) 583-598.

[53] Gottlieb P, Folgering J, Maroto R, *et al*. Revisiting TRPC1 and TRPC6 mechanosensitivity. *Pflugers Arch*. 455 (2007) 1097-1103.

[54] Iwata Y, Katanosaka Y, Arai Y, Shigekawa M and Wakabayashi S. Dominant negative inhibition of calcium influx via TRPV2 ameliorates muscular dystrophy in animal models. *Hum Mol Genet*. 18 (2009) 824-834.

[55] Suchyna TM and Sachs F. Mechanosensitive channel properties and membrane mechanics in mouse dystrophic myotubes. *J Physiol*. 581 (2007) 369-387.

[56] Hino N, Ochi R and Yanagisawa T. Inhibition of the slow inward current and the time-dependant outward current of mammalian ventricular muscle by gentamicin. *Pflugers Arch*. 394 (1982) 243-249

[57] Belus A and White E. Effects of streptomycin sulfate on I(CaL), I(Kr) and I(Ks) in guinea-pig ventricular myocytes. *Euro J Pharmacol*. 445 (2002) 171-178.

[58] Kamkin A, Kiseleva I and Isenberg G. Ion selectivity of stretch-activated cation currents in mouse ventricular myocytes. *Pflügers Arch.* 446 (2003) 220-231.

[59] Yang XC and Sachs F. Block of stretch-activated ion channel in Xenopus oocytes by gadolinium and calcium ions. *Science*. 243 (1989) 1068-1071.

[60] Jung C, Martins AS, Niggli E and Shirokova N. Dystrophic cardiomyopathy: amplification of cellular damage by Ca^{2+} signalling and reactive oxygen species-generating pathways. *Cardiovasc Res*. 77 (2007) 766-773.

[61] Copello JA, Zima AV, Diaz-Sylvester PL, Fill M and Blatter LA. Ca^{2+} entry-independant effects of L-type Ca^{2+} channel modulators on Ca^{2+} sparks in ventricular myocytes. *Am J Physiol Cell Physiol.* 292 (2007) C2129-C2140.

[62] Koch SE, Gao X, Haar L, *et al*. Probenecid: novel use as a non-injurious positive inotrope acting via cardiac TRPV2 stimulation. *J Mol Cell Cardiol*. 53 (2012) 134-144.